



ELSEVIER

Journal of Biomechanics ■ (■■■■) ■■■-■■■

JOURNAL  
OF  
BIOMECHANICSwww.elsevier.com/locate/jbiomech  
www.JBiomech.com

# A hypothesis for the function of braking forces during running turns

Devin L. Jindrich<sup>a,\*</sup>, Thor F. Besier<sup>b</sup>, David G. Lloyd<sup>c</sup><sup>a</sup>Department of Physiological Science, University of California, Los Angeles, 621 Charles E. Young Dr. South, Los Angeles, CA 90095-1761, USA<sup>b</sup>Biomechanical Engineering Division, Mechanical Engineering Department, Stanford University, Stanford, CA 94305-3030, USA<sup>c</sup>School of Human Movement and Exercise Science, University of Western Australia, 35 Stirling Highway, Crawley, WA 6009, Australia

Accepted 7 May 2005

## Abstract

We examined the functional role of braking forces observed when humans execute turning maneuvers. Deceleration caused by braking forces contributes to changing the movement direction of the center of mass (COM) and maintaining constant velocity. We argue that braking forces also prevent over-rotation of the body about the vertical axis during maneuvers. We analyzed data from sidestep and crossover cuts at average initial running velocities of  $3 \text{ ms}^{-1}$ . Absent braking, lateral forces would result in body rotations 1.4–3 times the change in COM movement direction, causing the orientation of the body to be substantially mis-aligned with the direction of movement at the end of the step. A simple model based on the hypothesis that body rotation should match COM deflection can explain 70% of the variance in braking forces employed during running turns.

© 2005 Published by Elsevier Ltd.

**Keywords:** Sidestepping; Cutting; Maneuverability; Navigation; Locomotion

## 1. Introduction

When executing turning or cutting maneuvers, humans generate braking forces. Braking is observed during both running (Besier et al., 2001a), and walking turns (Patla et al., 1991), and has been explained as contributing to turn sharpness by causing deceleration in the initial movement direction (Houck, 2003). For example, braking forces are required for  $90^\circ$  turns (Walter, 2003). However, for turn magnitudes less than  $90^\circ$ , deceleration is not necessary for changing the movement direction. Consequently, the functional role of braking when executing maneuvers is not fully understood.

Two mechanical requirements characterize turning maneuvers: the velocity of the center of mass (COM) must be changed to a new direction (“deflection”) and

the body must rotate to align with the new direction of motion (Jindrich and Full, 1999; Patla et al., 1991). Requirements for body rotation may constrain turning performance. For example, increasing yaw moment of inertia results in decreased turning ability and reduced speed during running maneuvers (Carrier et al., 2001).

We hypothesize that the requirement for body rotation about the vertical axis to match COM movement deflection at the end of a turn constrains leg force production during turning maneuvers. Specifically, we hypothesize that the forces required to deflect the COM during running would result in over-rotation of the body without production of additional braking forces. We analyzed ground-reaction force and kinematic data from subjects running and executing three types of cutting turns to test this hypothesis in two ways. First, we used a sinusoidal decomposition to separate braking forces associated with cutting from the deceleration/acceleration observed during constant-speed locomotion. We then estimated the body rotation that would have occurred without braking forces by removing the braking force component and double-integrating the

\*Corresponding author. Tel.: +1 310 825 9055; fax: +1 310 267 2071.

E-mail addresses: dljindrich@yahoo.com (D.L. Jindrich), besier@stanford.edu (T.F. Besier), dlloyd@cyllene.uwa.edu.au (D.G. Lloyd).

1 remaining forces in the horizontal plane. We compared  
 2 this estimated body rotation to the rotation observed  
 3 during the maneuver. Second, we developed a simple  
 4 model of maneuvering based on easily measured or  
 5 estimated morphological and behavioral parameters.  
 6 The model can predict the braking (or acceleratory)  
 7 forces necessary for body rotation to match movement  
 8 deflection, so that the velocity of movement at the end of  
 9 stance lies in the sagittal plane. We compared the  
 10 predictions of the model to the observed braking forces.

## 13 2. Methods

15 We analyzed force and kinematic data from seven  
 16 male subjects of mass ( $M$ )  $74 \pm 8$  kg. Informed consent  
 17 was gained before testing, and experiments were  
 18 approved by the ethics committee of the University of  
 19 Western Australia. Kinematic, ground reaction force  
 20 (GRF), and kinetic data were collected using a six-  
 21 camera, 50-Hz VICON motion analysis system (Oxford  
 22 Metrics Ltd., Oxford, UK) and a  $1200 \times 600$  mm force  
 23 plate at 2000 Hz (Advanced Mechanical Technology  
 24 Inc., Watertown, MA) as detailed previously (Besier  
 25 et al., 2001b). Subjects were instructed to run at  $3 \text{ m s}^{-1}$   
 26 and execute one of four tasks in response to a light cue:  
 27 RUN, straight-ahead running; S30, running sidesteps of  
 28  $30^\circ$ ; S60, sidesteps of  $60^\circ$ ; X30,  $30^\circ$  crossover cuts. The  
 29 order of the conditions was randomized. Previous  
 30 studies have identified different motor strategies under-  
 31 lying anticipated (where subjects have prior knowledge  
 32 of the turn direction) and unanticipated (where subjects  
 33 do not know the turn direction until immediately before  
 34 the turn) turns (Besier et al., 2001a). Since we seek to  
 35 characterize a wide range of maneuvers, we included  
 36 both anticipated and unanticipated turns in the analysis.  
 37 Kinematic and force data from the stance period of the  
 38 first step of the maneuver were isolated from 10 trials for  
 39 each subject and maneuver condition. COM location  
 40 was estimated as the mid-point between hip joint center  
 41 markers, and  $I$  was estimated as  $1.24 \text{ kg m}^2$  for a 78 kg  
 42 male scaled to  $M^{5/3}$  (Carrier et al., 2001).

43 During complex movements such as sidestepping or  
 44 crossover cutting, fore-aft and lateral axes may be  
 45 difficult to define. Consequently, we expressed kinematic  
 46 and force data in a coordinate system relative to the  
 47 initial movement direction (imd; Bauby and Kuo, 2000).

48 To estimate the amount of body rotation caused by  
 49 ground reaction forces in the transverse plane, sinusoid-  
 50 based equations were developed to represent the  
 51 component of force in the initial movement direction,  
 52  $F_{\text{imd}}(t)$  (Fig. 1A), and forces perpendicular to initial  
 53 movement direction,  $F_p(t)$ . The force in the initial  
 54 movement direction was decomposed into two sinusoi-  
 55 dal elements assumed to be linearly superimposed  
 during cutting. The first element ( $F_z(t)$ ), was a full-

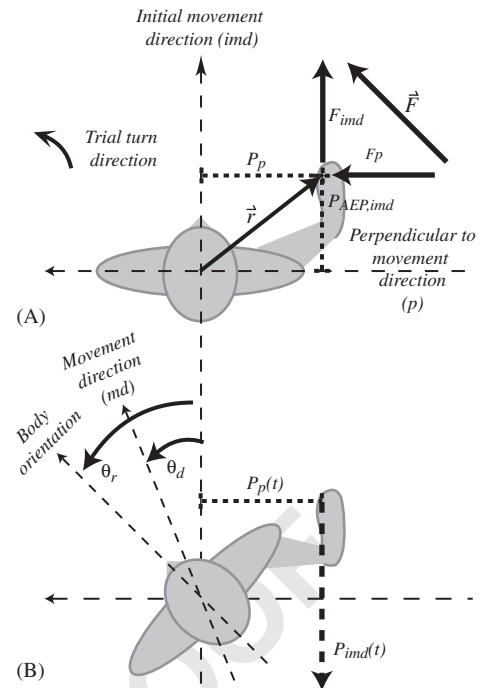


Fig. 1. Geometric variables used to describe turning maneuvers. (A) Schematic of kinematic and mechanical parameters measured at the beginning of stance. Vectors are expressed in a coordinate system based on the initial movement direction (imd). Positive values in the imd are up the page, and positive values perpendicular to the imd ( $p$ ) are to the left. (B) Rotation of the body and movement of the foot over time. Changes in body orientation ( $\theta_r$ ) and movement direction ( $\theta_d$ ) are calculated relative to values at the beginning of stance. For the simple turning model, foot position over time in the imd,  $P_{\text{imd}}(t)$ , was assumed to follow a linear path along the negative imd. Foot position over time perpendicular to the imd ( $P_p$ ) was assumed to be constant.

sinusoid that modeled the decelerating and accelerating forces normally observed during constant-average-speed locomotion (Cavagna et al., 1977). The second element ( $F_\beta(t)$ ), was a half-sinusoid modeling the additional braking forces associated with turning. Therefore, the  $F_{\text{imd}}(t)$  was represented using the equation

$$F_{\text{imd}}(t) = F_z(t) + F_\beta(t) = \alpha \sin\left(\frac{2\pi t}{\tau}\right) + \beta \sin\left(\frac{\pi t}{\tau}\right), \quad (1)$$

where  $t$  is time,  $\tau$  is the stance period and  $\alpha$  and  $\beta$  are peak forces (Fig. 2A). The force in the transverse plane perpendicular to initial movement direction,  $F_p(t)$ , was modeled as a half-sinusoid,

$$F_p(t) = F_{p\text{max}} \sin\left(\frac{\pi t}{\tau}\right). \quad (2)$$

For each trial, parameters  $\alpha$  and  $\beta$  in Eq. (1), and  $F_{p\text{max}}$  in Eq. (2) were fitted using a minimization algorithm (*fminsearch* in MATLAB R13, Mathworks, Natick, MA, USA).

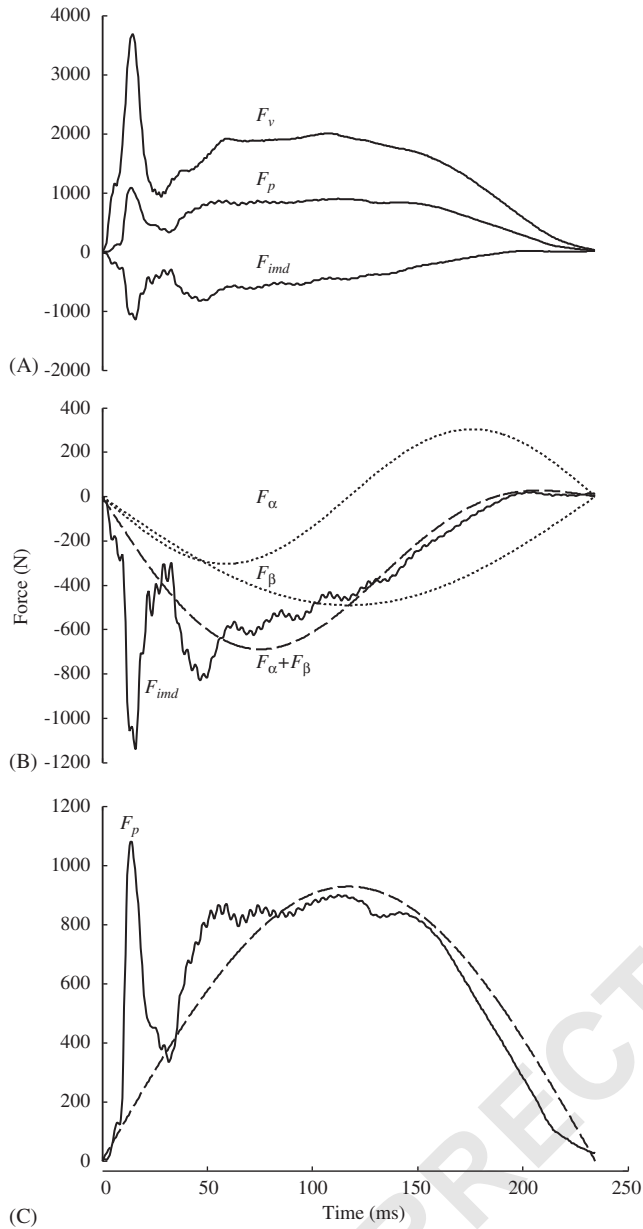


Fig. 2. Forces during the stance period of one sidestep cutting trial. (A) Vertical ( $F_v$ ), initial movement direction ( $F_{imd}$ ) and forces perpendicular to the initial movement direction ( $F_p$ ) during a representative maneuver. (B) Sinusoids  $F_\alpha$  and  $F_\beta$  (dotted lines) fitted to imd forces during the stance period. For this trial, the resulting superposition,  $F_\alpha + F_\beta$  accounted for 62% of the variance in  $F_{imd}$  over the entire step, and 82% after the first 50 ms. (C) Half-sinusoid fitted to  $F_p$ , which could account for 74% of the variance in force over the entire step, and 87% after the first 50 ms.

The body rotation ( $\theta_r$ ) was calculated using the equation

$$\theta_r = \int_0^\tau \int_0^\tau \frac{\vec{F}(t) \times \vec{r}(t) + T(t)}{I} dt + \dot{\theta}_i dt, \quad (3)$$

where  $\vec{r}$  was estimated as the vector between the COM and the center of pressure (COP; Fig. 1A) in the transverse plane,  $T(t)$  is the free moment about the vertical axis,  $I$  is the moment of inertia about the vertical axis, and  $\dot{\theta}_i$  is the rotational velocity about the vertical axis at the beginning of the step, which was estimated from differentiating the angle of a line connecting the hip joint centers with respect to time. The force vector in the transverse plane was  $\vec{F}(t) = F_{imd}(t) + F_p(t)$ .

The force vector,  $\vec{F}(t)$ , was different when examining the body rotation with or without braking forces. When determining the expected body rotation with braking forces ( $\theta_r^{wb}$ ), force in the initial movement direction,  $F_{imd}(t)$ , was set to  $F_\alpha(t) + F_\beta(t)$ . When the expected body rotation was estimated without the effect of braking forces ( $\theta_r^{wob}$ ; i.e. solely with the forces necessary to deflect the COM and the normal deceleration/acceleration forces),  $F_{imd}(t)$  was set to  $F_\alpha(t)$ . To evaluate whether braking forces prevent over-rotation of the body, we compared  $\theta_r^{wb}$  to  $\theta_r^{wob}$ .

To interpret the function of braking forces in a broader context, we developed a simple model of maneuverability that can be used to predict forces during turns based on morphological and behavioral parameters (Jindrich and Full, 1999). The model can be used to predict the braking forces necessary for body rotation to match movement deflection at the end of a maneuver, and a positive correlation between the model predictions and the measured braking force maxima  $\beta$  would provide further support for our hypothesis.

The model (see appendix for the mathematical development) assumes that a biped traveling at average velocity  $V$ , seeks to deflect the direction of movement by  $\theta_d$  during a step (Fig. 1B). At the beginning of the step, the foot is placed at an anterior extreme position parallel to the initial movement direction ( $P_{AEP,imd}$ ; Fig. 1A), and generates a sinusoidal lateral force for the duration of stance. If the foot is not placed directly lateral to the COM, generating the lateral impulse necessary to change the movement direction will result in a torque that causes the body to rotate by  $\theta_p$ . The proportion to which body rotation caused by  $F_p(t)$  matches movement deflection can be estimated by a “leg effectiveness number”,

$$\varepsilon = \frac{\theta_p}{\theta_d} = \frac{MV\tau}{2I} \left( P_{AEP,imd} - \frac{4V\tau}{\pi^2} \right). \quad (4)$$

An  $\varepsilon$  of 1 indicates that the leg is favorably placed for rotation to match deflection at the end of the step period, given the desired maneuver and the body shape. An  $\varepsilon > 1$  indicates that the body will tend to over-rotate, an  $\varepsilon < 1$  indicates that the body will under-rotate.

If  $\varepsilon$  does not equal 1, a fore-aft force can prevent over-rotation or compensate for under-rotation. The maximum ( $F_{h,max}$ ) of a half-sinusoidal fore-aft force necessary to prevent over-rotation or compensate for

under-rotation can be predicted as

$$F_{h\max} = \frac{\pi I(1 - \varepsilon)\theta_d}{\tau^2 P_p}, \quad (5)$$

(Jindrich and Full, 1999), where  $P_p$  is the lateral foot placement, calculated as the average distance from the COM to the center of pressure (COP; see below) perpendicular to the imd. To test whether this simple model can capture the mechanics of sidestep and crossover cutting, we used Eqs. (4) and (5), given  $V$ ,  $\tau$ ,  $P_{AEP,imd}$  and  $P_p$  for each trial, to predict  $F_{h\max}$ , and compared  $F_{h\max}$  to the fitted braking force maxima  $\beta$ .

We calculated the resultant COM velocity over the stride by differentiating the measured COM position in the horizontal plane using a fourth-order difference equation (Blickhan and Full, 1992); the initial velocity,  $V_i$ , was calculated as the instantaneous speed at the beginning of stance,  $V_{\text{stance}}$ , as the average speed during stance, and the final velocity as the instantaneous speed at the end of stance. The velocity,  $V$ , in Eq. (4) was set to  $V_i$ . The stance period,  $\tau$ , was determined as the time between vertical force onset ( $F_v > 1\text{ N}$ ) and force offset ( $F_v < 1\text{ N}$ ). The deflection of the COM,  $\theta_d$ , was calculated by integrating the horizontal ground-reaction force over stance, adding this velocity change to the initial velocity, and calculating the angle between final and initial velocity.

To estimate the foot placement,  $P_{AEP,imd}$  and  $P_p$ , the mean distance from a marker placed above the head of the second metatarsal to the COP was first calculated over the entire step for each trial. These values were then averaged for each condition and subject, and averaged again across subjects to yield a mean value for the metatarsal-COP distance for each condition. For each trial,  $P_{AEP,imd}$  was then calculated as the distance from the COM to the expected position of the mean COP relative to the toe marker in the initial movement direction (with an equivalent calculation for  $P_p$ ). These calculations served to minimize noise due to force transients at foot impact, and evaluate the potential of the model to predict braking forces based solely on kinematic measurements (see Discussion).

For each trial, we evaluated  $\varepsilon$  using Eq. (3), and predicted  $F_{h\max}$  using Eq. (4). Parameters measured during turning were compared using a repeated-measures ANOVA, with maneuver type as a fixed effect and subject as a random effect, using a computer statistics program (JMP 4.0.2, SAS Institute Inc., Cary, NC). Tukey post-hoc tests with significance values of 0.05 were used for comparisons among maneuver types. Data from the 10 trials analyzed from each subject and condition were averaged, and reported as means  $\pm$  standard deviations across subjects.

### 3. Results

Braking forces acted to prevent over-rotation of the body during sidestep and crossover cutting maneuvers. Without braking forces, body rotations would be 140–300% of the deflection of the movement direction for the three turning conditions ( $\frac{\theta^{\text{wob}}}{\theta^{\text{wb}}}$ ; Table 1). This over-rotation would result in a mis-alignment of the body axis with the movement direction at the end of the step. Expected body rotation without braking was significantly greater than rotation with braking forces for the S30, X30, and S60 ( $t$ -test,  $P < 0.01$ ), but not for the RUN condition ( $P > 0.8$ ).

Sinusoidal reconstructions of imd forces accounted for  $64 \pm 11\%$  of the variance in  $F_{imd}(t)$  over the entire step. Transients associated with leg impact in the first 50 ms of stance were not captured (Fig. 2B). After the first 50 ms of stance, reconstructions accounted for  $78 \pm 6\%$  of  $F_{imd}(t)$ . Excluding straight running trials (where lateral forces are of small magnitude and variable) and only considering sidestep and crossover cutting trials, a half-sinusoid fitted to  $F_p(t)$  could account for  $75 \pm 8\%$  over the entire stance period, and  $86 \pm 4\%$  after the first 50 ms.

The mean COP position relative to the head of the second metatarsal showed significant differences among conditions (Table 1). The COP moved posteriorly and medially for the sidestep turns (S30 and S60) relative to running, and laterally for crosscut maneuvers (X30).

Measured braking forces were directly related to deflection (Fig. 3A), but did not show clear correlations with other measured parameters, including velocity, foot placement, and stance period, as indicated by  $r^2$  values less than 0.37 (Fig. 3B–E). Direct prediction of expected braking forces for each trial were only possible by considering the mechanical parameters together using Eqs. (4) and (5). Leg effectiveness,  $\varepsilon$ , ranged from  $2.0 \pm 0.8$  for the X30 turns, to  $4.2 \pm 1.0$  for S60 turns, suggesting that over-rotation would be expected in the absence of braking forces. Measured braking forces were linearly related to the braking forces ( $F_{h\max}$ ) predicted from  $\varepsilon$  (Fig. 3F). The slope of a least-squares regression was 0.97, approximately a 1-to-1 relationship. The correspondence between measured braking forces and forces predicted to be required to prevent over-rotation provides additional support for the hypothesis that braking forces act to prevent over-rotation.

### 4. Discussion

Without braking forces, the body rotation during stance would be 1.4–3 times greater than the measured COM deflection, resulting in a substantial mis-alignment of body orientation and movement direction. Moreover, a simple model based on the assumption that

Table 1  
Parameters measured during four experimental conditions

Condition	RUN	S30	X30	S60
Full-sine component fitted to imd force, $\alpha$ (N)	$-214 \pm 44$ (S60)	$-230 \pm 40$ (S60)	$-220 \pm 46$ (S60)	$-259 \pm 50$
Half-sine component fitted to imd force, $\beta$ (N)	$17 \pm 45$ (S30,X30,S60)	$-161 \pm 73$ (X30,S60)	$-130 \pm 80$ (S60)	$-327 \pm 91$
Maximum fitted perpendicular force, $F_{p\max}$ (N)	$32 \pm 45$ (S30,X30,S60)	$600 \pm 114$ (X30,S60)	$-499 \pm 137$ (S60)	$669 \pm 158$
Ratio of rotation without braking to rotation with braking, $\frac{\theta_r^{\text{wob}}}{\theta_r^{\text{wb}}}$ (%)	$113 \pm 19$ (S30,S60)	$189 \pm 4$ (X30,S60)	$138 \pm 22$ (S60)	$295 \pm 62$
Initial velocity, $V_i$ ( $\text{m s}^{-1}$ )	$3.1 \pm 0.1$ (S30,X30,S60)	$3.0 \pm 0.2$ (S60)	$3.0 \pm 0.2$	$2.9 \pm 0.2$
Velocity during stance, $V_{\text{stance}}$ ( $\text{m s}^{-1}$ )	$2.9 \pm 0.1$ (S30,X30,S60)	$2.6 \pm 0.2$ (X30,S60)	$2.7 \pm 0.1$ (S60)	$2.3 \pm 0.2$
Stance period, $\tau$ (s)	$0.258 \pm 0.031$ (S60)	$0.269 \pm 0.032$ (S60)	$0.267 \pm 0.035$ (S60)	$0.302 \pm 0.038$
Mean COP position relative to head of second metatarsal, initial movement direction (mm)	$-9 \pm 8$ (S30,S60)	$-19 \pm 11$ (S60)	$-15 \pm 12$ (S60)	$-31 \pm 11$
Mean COP position relative to head of second metatarsal, perpendicular to imd (mm)	$-25 \pm 18$ (S30,X30,S60)	$2 \pm 15$ (X30)	$-51 \pm 28$ (S60)	$-6 \pm 33$
Anterior extreme foot placement in initial movement direction, $P_{\text{AEP, imd}}$ (m)	$0.33 \pm 0.04$ (S30,X30,S60)	$0.39 \pm 0.04$ (S60)	$0.38 \pm 0.03$ (S60)	$0.46 \pm 0.05$
Foot placement perpendicular to movement direction, $P_p$ (m)	$-0.04 \pm 0.02$ (S30,X30,S60)	$-0.25 \pm 0.02$ (X30)	$0.15 \pm 0.05$ (S60)	$-0.27 \pm 0.01$
COM deflection, $\theta_d$ (degrees)	$3 \pm 1$ (S30,X30,S60)	$28 \pm 1$ (X30,S60)	$-24 \pm 4$ (S60)	$42 \pm 5$
Leg effectiveness, $\varepsilon$	$0.82 \pm 0.7$ (S30,X30,S60)	$2.5 \pm 0.7$ (X30,S60)	$2.0 \pm 0.8$ (S60)	$4.2 \pm 1.0$
Predicted forces in movement direction, $F_{h\max}$ (N)	$-12 \pm 108$ (S30,X30,S60)	$-118 \pm 55$ (S60)	$-84 \pm 69$ (S60)	$-259 \pm 88$

Values are means  $\pm$  standard deviations. Significant differences among conditions are indicated in parentheses.

body rotation should match movement deflection predicted measured braking forces during running turns of different types. These findings support the hypothesis that braking forces prevent over-rotation during running turns.

Several experimental limitations should be considered when interpreting the results. First, impact forces that are observed in running and cutting were not modeled. Impact forces may be associated with injury, and should be considered when evaluating the potential for leg injury during different activities (Nigg and Wakeling, 2001). However, the mechanical predictions based on modeling solely “active” forces as we have may also apply to impact forces. In the conditions used in this study vertical, fore-aft, and lateral impact forces showed close correlations to active force peaks over different turn magnitudes. Comparing the first ground-reaction vertical force peak,  $F_{\text{faimpact}}$ , to the second peak,  $F_{\text{faactive}}$ , yielded the relationship  $F_{\text{faimpact}} = 1.2F_{\text{faactive}} - 222$ ;  $R^2 = 0.996$ . Impact forces are associated with decelerating the leg segments upon contact with the ground (Nigg et al., 1987). Assessing the effects of impact forces on movements of the COM, which are the primary concern of this study, would require an inverse-dynamics model of the leg and body. To make a simple

approximation of the potential errors, we double-integrated the rotational accelerations due to horizontal-plane impact forces. Potential body rotations due to impact forces were  $-5 \pm 4^\circ$ ,  $3 \pm 9^\circ$ ,  $2 \pm 11^\circ$ , and  $-23 \pm 13^\circ$  for the RUN, S30, S60, and X30 conditions, respectively. In the straight-running and sidestep cutting conditions, potential effects of impact forces were small. The larger potential error in the X30 condition can be explained by forces due to the added inertia when the leg is swung across the body for crossover cuts. Although these calculations suggest that impact forces may not substantially impact body rotation during turns, additional experiments will be required to fully assess the role of impact forces during maneuvers.

Second, the kinematic data did not include markers for the trunk and arms. Instantaneous trunk and limb position could also affect COM location and  $I$ , but were assumed constant during stance. Trunk lean in the roll and pitch directions could affect turning requirements. For example, lean would increase  $I$  about the vertical axis, since trunk  $I$  in the sagittal and transverse planes are greater than in the longitudinal plane (de Leva, 1996). The moment of inertia values used in the current analysis may therefore underestimate  $I$ . Underestimating  $I$  would not change the ratio  $\frac{\theta_r^{\text{wob}}}{\theta_r^{\text{wb}}}$ , since both angles

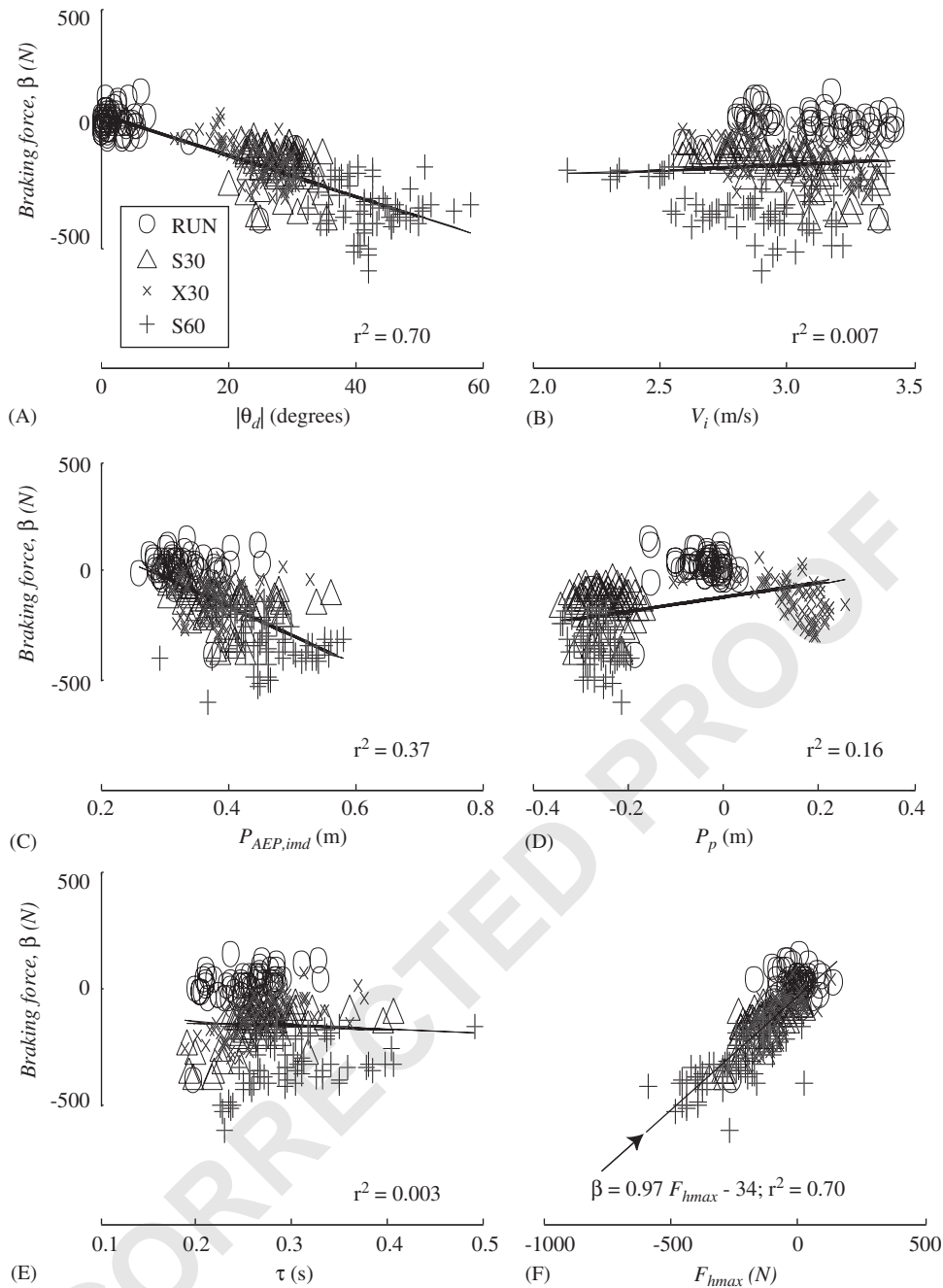


Fig. 3. Relationship of braking forces to turning parameters. Measured values of braking forces ( $\beta$ ) plotted against deflection magnitude ( $|\theta_d|$ ; A), initial velocity ( $V_i$ ; B), initial foot placement in the initial movement direction ( $P_{AEP,imd}$ ; C), and perpendicular to the initial movement direction ( $P_p$ ; D) and stance period ( $\tau$ ; E). (F)  $\beta$  plotted against predicted values of  $F_{hmax}$  calculated from Eqs. (3) and (4).

are equally dependent on  $I$ . However, the leg effectiveness number,  $\varepsilon$ , is directly related to  $I^{-1}$  (Eq. 4). Based on the inertial parameters reported in de Leva (1996), we estimate that a roll lean of  $55^\circ$  would be necessary to calculate an  $\varepsilon$  of 1 ( $F_{hmax} = 0$ ) in the X30 condition, and braking forces would be required even in the case of a  $90^\circ$  trunk lean in the S60 condition. Consequently, we consider it unlikely that considering trunk and limb positions would change the conclusions of the study.

In addition to moments about the COM caused by ground-reaction forces, humans may also generate free moments based on force couples at the foot (Holden and Cavanagh, 1991). During RUN trials, normalized angular impulses due to free moments of  $-5.4 \pm 7.7 \text{ s } 10^{-4}$  were of similar magnitude, but opposite direction of the angular impulses of  $4.7 \text{ s } 10^{-4}$  measured by Holden and Cavanagh (1991). This discrepancy could be due to the fact that Holden and

Cavanagh (1991) selected rearfoot strikers who wore running shoes, whereas in the present study runners were barefoot, and frequently executed turns using toe strikes. Free moment magnitudes increased to  $-17.8 \pm 5.9 \text{ s } 10^{-4}$  and  $-22.6 \pm 8.2 \text{ s } 10^{-4}$  for S30 and S60 conditions, respectively, and decreased to  $-2.8 \pm 8.3 \text{ s } 10^{-4}$  for the X30 condition. These negative free moments acted against over-rotation, but were only  $16\% \pm 6\%$ ,  $8\% \pm 5\%$ , and  $10\% \pm 2\%$  of the moments due to  $F_p$  for the S30, X30 and S60 conditions, respectively. Although we selected barefoot running to avoid the potential effects of shoes on cutting strategy and mechanics, it represents only one locomotor condition. Future studies will be necessary to determine the impact of shoes, and shoe design, on maneuverability.

Active force peaks in the initial movement direction during running turns were modeled as the superposition of half-sinusoidal forces onto the imd forces observed during straight running. Measured values for  $\alpha$  of  $214 \pm 44$  were within 15% and 10% of peak propulsive and braking forces observed during constant-velocity locomotion at  $3.3 \text{ m s}^{-1}$  ( $193 \pm 7$  and  $227 \pm 6.6 \text{ N}$ , respectively; Chang and Kram, 1999).

Both direct estimation of body rotation and the simple maneuvering model suggest that body over-rotation is a potential problem during cutting turns. Several implications emerge from the concept of leg “effectiveness” presented in Eq. (4). The multiplicand, which expresses foot placement,  $P_{\text{AEP,imd}}$ , relative to the movement of the foot during stance (determined by  $V$  and  $\tau$ ) is important, since it is a major factor in determining whether braking or acceleration is necessary to maintain body orientation aligned with COM deflection at the end of stance. Initial velocity,  $\tau$ , and  $I$  scale the magnitude of required force. Behavioral changes, such as adopting a crouched posture, could reduce required forces by increasing  $I$ .

Subjects altered several movement parameters to execute different types of turns. The most pronounced adjustment made during cutting was an increased lateral foot placement,  $P_p$ . The magnitude of  $P_p$  increased from 4 cm during running, to 25 and 27 cm for the S30 and S60 conditions, respectively (Table 1). In contrast, more modest changes in  $P_{\text{AEP,imd}}$  were observed. It was surprising that  $P_{\text{AEP,imd}}$  increased to 46 cm during the S60 condition, considering that increases in  $P_{\text{AEP,imd}}$  would be expected to result in increased over-rotation.

Increasing turn magnitude from S30 to S60 was associated with increased  $\theta_d$  and  $F_{p\text{max}}$  (Table 1). However, despite the goal of doubling the turn magnitude from  $30^\circ$  to  $60^\circ$ ,  $\theta_d$  only increased by 50% to an average value of  $42^\circ$  during the measured stance period. The S60 condition may approach maximum performance for turns at  $3 \text{ m s}^{-1}$  running speeds, and completely executing the task may have required more

than a single step. This is supported by the modest increase, 11%, in  $F_{p\text{max}}$  in the S60 condition relative to the S30 condition. Instead of increasing lateral forces, subjects increased  $\tau$ , as predicted for maximum-effort turns (Greene, 1985).

Over multiple steps of both maximum- and sub-maximum effort maneuvers, decreases in running speed are often observed (Besier et al., 2001b; Greene, 1985). Limitations to maximum leg forces may limit running speed during maximum effort curve running (Greene, 1985), but would not be expected to result in speed decreases during sub-maximal curve running. Surprisingly, the decreases in velocity over the entire trials did not appear to be related to braking forces during the first step of cutting maneuvers. Deceleration in the initial movement direction was offset by acceleration perpendicular to the movement direction, resulting in an average final velocity over all conditions of  $2.95 \pm 0.24 \text{ m s}^{-1}$  which was the same as the initial velocity of  $2.95 \pm 0.22 \text{ m s}^{-1}$ . During running turns, the inside leg has been implicated as contributing to speed decreases (Chang et al., 2001), and crossover cuts may be similar to steps of the inside leg during running turns. However, speed decreases were not observed during crossover cuts. Final velocities of  $3.06 \pm 0.15 \text{ m s}^{-1}$  were not significantly different from initial velocities of  $3.02 \pm 0.19 \text{ m s}^{-1}$ . However, increasing turn magnitude was associated with decreases in  $V_{\text{stance}}$  (Table 1), and final velocity for the S60 condition of  $2.73 \pm 0.21 \text{ m s}^{-1}$  was less than the initial velocity of  $2.86 \pm 0.25 \text{ m s}^{-1}$ , although this difference was not significant. Other factors, such as motivational factors or stability requirements, may result in decreases in speed following sidestep and crossover cuts.

When executing crossover cuts, subjects adjusted their foot position medially, resulting in a foot placement approaching that which would be used by the opposite leg executing a sidestep turn. Nevertheless, the leg effectiveness allowed braking forces to be predicted for crossover cutting (Fig. 3F). The ability of the model to estimate braking forces during crossover cuts was surprising considering the large differences in body geometry and kinematics required.

A potential application of this simple model is to predict forces during maneuvers in settings where ground-reaction force measurements may not be available. Most of the model parameters can be measured from anthropometry or kinematic measurements. Ideally, the foot placement parameters  $P_{\text{AEP,imd}}$  and  $P_p$  represent the distance between COM and COP. In the experiments reported here we found that using the mean COP position relative to a toe marker at the head of the second metatarsal represented a reasonable surrogate for the COP.

Braking forces are not limited to running sidesteps, but also observed during walking turns executed at less

than half of the speed used by subjects in the present study (Houck, 2003; Patla et al., 1991). At lower speeds, lateral forces are less than those during running, stance periods are increased, and there may be more opportunity to generate free moments to prevent under- or over-rotation during turns. To estimate whether over-rotation may be expected to occur without braking forces during walking turns, we calculated  $\varepsilon$ , and compared predicted  $F_{h\max}$  to measured braking forces from two studies: Patla et al. (1991) and Houck (2003). For Patla et al. (1991),  $\theta_d$  was  $60^\circ$ , average  $\tau$  was 0.53 s,  $P_{AEP,imd}$  was estimated from the step length (assuming a symmetric stride) as 0.4 m, and  $V_i$  as  $1.5\text{ m s}^{-1}$ . For Houck (2003),  $\theta_d$  was  $40^\circ$ , average  $\tau$  was 0.67 s,  $V_i$  was  $1.34\text{ m s}^{-1}$ .  $P_{AEP,imd}$  was estimated from the  $V_i$  and  $\tau$  (assuming a symmetric stride) as 0.45 m. Lateral foot placement,  $P_p$  was estimated as 0.18 m for the  $60^\circ$  turn and 0.15 m for the  $40^\circ$  turn (Courtine and Schieppati, 2003).

Average  $\varepsilon$  was estimated to be 1.8 for turns measured by Patla et al. (1991) and 2.3 for those reported by Houck (2003), indicating that absent braking forces, over-rotation may be expected even during turns at walking speeds. The  $F_{h\max}$  values of  $-65$  and  $-51$  N predicted using Eq. (4) were 112% and 150% of the measured peak braking forces of  $-58$  and  $-34$  N, respectively. Considering the difficulties introduced when using mean data for parameters that may co-vary, we consider these predictions to be suggestive that braking forces also act to prevent over-rotation during walking turns.

Analysis of kinematics and ground-reaction forces during sidestep and crossover cutting support the hypothesis that braking forces act to prevent over-rotation during running turns. Moreover, a simple model based on this hypothesis can predict ground-reaction forces based on a limited number of measured parameters. Future studies to relate ground-reaction forces to knee loading could afford predictions of knee injury risks during maneuvers based on a small set of morphological and kinematic parameters, since braking forces may be associated with increased risk (Colby et al., 2000; Houck, 2003). For example, in sidestepping maneuvers when perpendicular ( $F_p(t)$ ) and braking ( $F_\beta(t)$ ) forces peak during the push-off phase as defined by Besier et al. (2001a,b), the internal rotation moments on the knee also reached their peak values (Besier et al., 2001a,b). Peak push-off was suggested to be a phase where there was a high risk of anterior cruciate ligament injuries. Peak push-off is during the active phase where the current model best predicts the transverse plane ground-reaction forces. Although it could be speculated that the degree of potential over-rotation may influence the size of the internal rotation moments at the knee, additional experiments will be necessary to determine the relationship between the ground-reaction forces

predicted by this simple model, impact forces, and knee loading specifically associated with this injury. In addition to better understanding direct causes of injury, characterizing maneuverability is important because of its impact on stability. For example, turning is associated with increased risks of falling and subsequent injury (Thigpen, et al., 2000). Characterizing the mechanical constraints for maneuvers under varying conditions can contribute to understanding of the control strategies necessary for stable locomotion.

### Acknowledgments

The authors would like to thank Young-Hui Chang, Craig McGowan and Eileen Kim for critically reading the manuscript.

### Appendix

We seek to make testable predictions of ground-reaction forces during turning maneuvers based on few, easily measured parameters. To this end, we developed a 2-dimensional (horizontal plane) model of turning. Several aspects of the model were simplified in the interest of deriving algebraic expressions which are clear, and provide the most intuitive embodiment possible. First, the model does not account for motions of the trunk (i.e. pitch or lean), and possible changes to moment of inertia ( $I$ ) which could result. Second, ground-reaction forces are considered to be sinusoidal in time, and do not include forces associated with leg impact. Third, the potentially complex trajectory of the foot relative to the COM during stance is simplified. The foot is assumed to move linearly relative to the COM in the initial movement direction (imd), and maintain a constant position perpendicular to the imd (Fig. 3B). During the three conditions studied, the position of the foot in the movement direction relative to the COM over time ( $P_{imd}$ ) was well approximated by a line. Linear fits to  $P_{imd}$  over time for each trial had  $r^2$  values of  $0.98 \pm 0.06$  for the S30 and X30 conditions, and  $0.97 \pm 0.08$  for the S60 condition. Foot position perpendicular to the imd ( $P_p$ ) was not constant, but increased over the turning step (Fig. A.1). However, sinusoidal forces are likely to reach maxima close to the average  $P_p$  used in the model, minimizing errors due to changing lateral foot position over the step.

### Leg Effectiveness

When executing a turn,  $P_{imd}$  is modeled as moving backwards at constant velocity ( $V$ ) from its initial placement at the anterior extreme position ( $P_{AEP,imd}$ ):

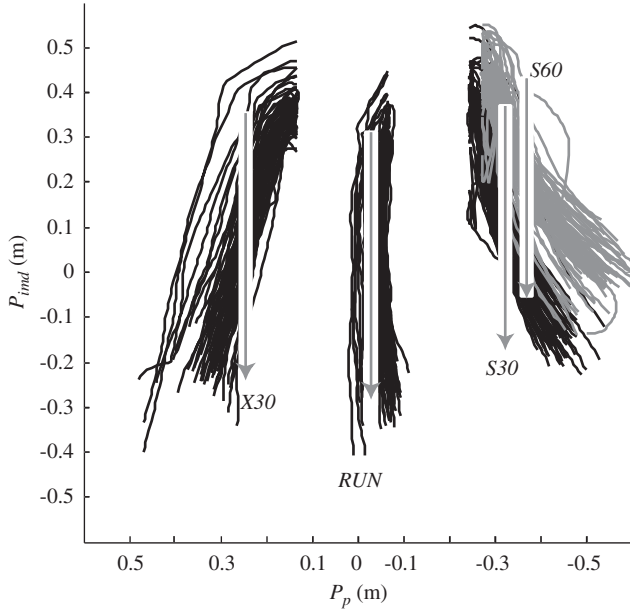


Fig. A.1. Foot position relative to the COM during running and cutting maneuvers. Vertical gray arrows are schematics of simplified foot trajectories used for turning model. Foot trajectories for S60 trials are shown in gray for clarity.

$$P_{\text{imd}}(t) = (P_{\text{AEP,imd}} - Vt). \quad (\text{A.1})$$

The component of force perpendicular to the movement direction ( $F_p$ ) is modeled as a half-sinusoid with period equal to the stance period  $\tau$ :

$$F_p(t) = F_{p \text{ max}} \sin\left(\frac{\pi t}{\tau}\right). \quad (\text{A.2})$$

The torque ( $T_p(t)$ ) is the product of the foot position and  $F_p(t)$ ,

$$T_p(t) = F_p(t)P_{\text{imd}}(t). \quad (\text{A.3})$$

Body rotation due to the perpendicular force necessary to deflect the movement direction ( $\theta_p$ ) can be calculated as the double integral of acceleration due to  $T_p$  with respect to time:

$$\begin{aligned} \theta_p &= \int_{t=0}^{t=\tau} \int_{t=0}^{t=\tau} \frac{T_p(t)}{I} dt dt \\ &= \int_{t=0}^{t=\tau} \int_{t=0}^{t=\tau} \frac{F_p(t)P_{\text{imd}}(t)}{I} dt dt \\ &= \int_{t=0}^{t=\tau} \int_{t=0}^{t=\tau} \frac{F_{p \text{ max}} \sin\left(\frac{\pi t}{\tau}\right) (P_{\text{AEP,imd}} - Vt)}{I} dt dt. \end{aligned} \quad (\text{A.4})$$

Integrating twice yields

$$\begin{aligned} \theta_p &= \frac{-P_{\text{AEP,imd}}F_{p \text{ max}}\tau^2 \sin\left(\frac{\pi t}{\tau}\right) + VtF_{p \text{ max}}\tau^2 \sin\left(\frac{\pi t}{\tau}\right) + \frac{2VF_{p \text{ max}}\tau^3}{\pi} \cos\left(\frac{\pi t}{\tau}\right)}{\pi^2 I} \\ &\quad + \frac{P_{\text{AEP,imd}}F_{p \text{ max}}\tau t}{\pi I} - \frac{2VF_{p \text{ max}}\tau^3}{\pi^3 I}. \end{aligned} \quad (\text{A.5})$$

For the definite integral  $\{t = 0, \tau\}$

$$\begin{aligned} \theta_p &= -\frac{2VF_{p \text{ max}}\tau^3}{\pi^3 I} + \frac{P_{\text{AEP,imd}}F_{p \text{ max}}\tau^2}{\pi I} - \frac{VF_{p \text{ max}}\tau^3}{\pi I} \\ &\quad - \frac{2VF_{p \text{ max}}\tau^3}{\pi^3 I}, \end{aligned} \quad (\text{A.6})$$

which can be simplified to

$$\theta_p = \frac{F_{p \text{ max}}\tau^2}{\pi I} \left( P_{\text{AEP,imd}} - \frac{4V\tau}{\pi^2} \right). \quad (\text{A.7})$$

If  $V$  remains constant, the change in momentum of the COM perpendicular to the imd equals the perpendicular force impulse over the step:

$$MV \sin(\theta_d) = \int_{t=0}^{t=\tau} F_p(t) dt. \quad (\text{A.8})$$

Considering sinusoidal force production,

$$\begin{aligned} MV \sin(\theta_d) &= \int_{t=0}^{t=\tau} F_{p \text{ max}} \sin\left(\frac{\pi t}{\tau}\right) dt \\ &= \left[ -\frac{F_{p \text{ max}}\tau}{\pi} \cos\left(\frac{\pi t}{\tau}\right) \right]_{t=0}^{t=\tau}, \end{aligned} \quad (\text{A.9})$$

which evaluates to

$$MV \sin(\theta_d) = \frac{2F_{p \text{ max}}\tau}{\pi}. \quad (\text{A.10})$$

Rearranging Eq. (A.10) allows  $F_{p \text{ max}}$  to be estimated as

$$F_{p \text{ max}} = \frac{\pi MV \sin(\theta_d)}{2\tau}. \quad (\text{A.11})$$

Substituting Eq. (A.11) into Eq. (A.7) yields

$$\theta_p = \frac{MV \sin(\theta_d)\tau}{2I} \left( P_{\text{AEP,imd}} - \frac{4V\tau}{\pi^2} \right). \quad (\text{A.12})$$

Normalizing both sides of this equation to  $\theta_d$  results in:

$$\frac{\theta_p}{\theta_d} = \frac{MV \sin(\theta_d)\tau}{2I\theta_d} \left( P_{\text{AEP,imd}} - \frac{4V\tau}{\pi^2} \right). \quad (\text{A.13})$$

For small angles,  $\frac{\sin(\theta_d)}{\theta_d} \approx 1$ . At the highest values for  $\theta_d$  measured for the S60 condition of  $42^\circ$ ,  $\frac{\sin(\theta_d)}{\theta_d} = 0.91$ . Consequently, we chose to use the additional approximation,  $\frac{\sin(\theta_d)}{\theta_d} = 1$ .

With this approximation, Eq. (A.13) can be re-written as the leg effectiveness number presented in Eq. (4):

$$\frac{\theta_p}{\theta_d} = \frac{MV\tau}{2I} \left( P_{\text{AEP,imd}} - \frac{4V\tau}{\pi^2} \right). \quad (\text{A.14})$$

*Braking forces*

For rotation to match deflection at the end of the step,  $\theta_d - \theta_p$  must equal zero, or alternatively  $(1 - \varepsilon)\theta_d = 0$ . The peak braking force,  $F_{h \text{ max}}$ , can be related to the leg effectiveness number by considering that the rotation due to  $F_h(t)$  must account for the under- or over-

rotation,  $\theta_d - \theta_p$ . If the braking force required for rotation to match deflection is modeled as a half-sine,

$$F_h(t) = F_{h \max} \sin\left(\frac{\pi t}{\tau}\right), \quad (\text{A.15})$$

$$\begin{aligned} (1 - \varepsilon)\theta_d &= \int_{t=0}^{t=\tau} \int_{t=0}^{t=\tau} \frac{F_h(t)P_p}{I} dt dt \\ &= \int_{t=0}^{t=\tau} \int_{t=0}^{t=\tau} \frac{F_{h \max} \sin\left(\frac{\pi t}{\tau}\right)P_p}{I} dt dt. \end{aligned} \quad (\text{A.16})$$

Evaluating the integrals yields

$$(1 - \varepsilon)\theta_d = \frac{F_{h \max} t \tau P_p}{\pi I} - \frac{F_{h \max} \tau^2 \sin\left(\frac{\pi t}{\tau}\right)P_p}{\pi^2 I} + C. \quad (\text{A.17})$$

Assuming initially zero angular position,  $C = 0$ . At  $t = \tau$

$$(1 - \varepsilon)\theta_d = \frac{F_{h \max} \tau^2 P_p}{\pi I}, \quad (\text{A.18})$$

which can be rearranged to Eq. (5):

$$F_{h \max} = \frac{\pi I (1 - \varepsilon) \theta_d}{\tau^2 P_p}. \quad (\text{A.19})$$

## References

- Bauby, C.E., Kuo, A.D., 2000. Active control of lateral balance in human walking. *Journal of Biomechanics* 33, 1433–1440.
- Besier, T.F., Lloyd, D.G., Ackland, T.R., Cochrane, J.L., 2001a. Anticipatory effects on knee joint loading during running and cutting maneuvers. *Medicine and Science in Sports and Exercise* 33, 1176–1181.
- Besier, T.F., Lloyd, D.G., Cochrane, J.L., Ackland, T.R., 2001b. External loading of the knee joint during running and cutting maneuvers. *Medicine and Science in Sports and Exercise* 33, 1168–1175.
- Blickhan, R., Full, R.J., 1992. Mechanical work in terrestrial locomotion. In: Biewener, A.A. (Ed.), *Biomechanics: Structures and Systems, a Practical Approach*. IRL Press at Oxford University Press, Oxford, pp. 75–96.

- Carrier, D.R., Walter, R.M., Lee, D.V., 2001. Influence of rotational inertia on turning performance of theropod dinosaurs: clues from humans with increased rotational inertia. *Journal of Experimental Biology* 204, 3917–3926. 41
- Cavagna, G.A., Heglund, N.C., Taylor, C.R., 1977. Walking, running and galloping: mechanical similarities between different animals. In: Pedley, T.J. (Ed.), *Scale effects in animal locomotion*. Academic Press, Cambridge, pp. 111–125. 43
- Chang, Y.H., Campbell, K., Kram, R., 2001. Running speed on curved paths is limited by inside leg. *Proceedings of the 25th Annual Meeting of the American Society of Biomechanics*, pp. 435–436. 45
- Chang, Y.H., Kram, R., 1999. Metabolic cost of generating horizontal forces during human running. *Journal of Applied Physiology* 86, 1657–1662. 47
- Colby, S., Francisco, A., Yu, B., Kirkendall, D., Finch, M., Garrett, W., 2000. Electromyographic and kinematic analysis of cutting maneuvers. *American Journal of Sports Medicine* 28, 234–240. 49
- Courtine, G., Schieppati, M., 2003. Human walking along a curved path. I. Body trajectory, segment orientation and the effect of vision. *European Journal of Neuroscience* 18, 177–190. 51
- de Leva, P., 1996. Adjustments to Zatsiorsky-Seluyanov's segment inertia parameters. *Journal of Biomechanics* 29, 1223–1230. 53
- Greene, P.R., 1985. Running on flat turns: experiments, theory, and applications. *Biomechanical Engineering* 107, 96–103. 55
- Holden, J.P., Cavanagh, P.R., 1991. The free moment of ground reaction in distance running and its changes with pronation. *Journal of Biomechanics* 24, 887–897. 57
- Houck, J., 2003. Muscle activation patterns of selected lower extremity muscles during stepping and cutting tasks. *Journal of Electromyography and Kinesiology* 13, 545–554. 59
- Jindrich, D.L., Full, R.J., 1999. Many-legged maneuverability: dynamics of turning in hexapods. *Journal of experimental Biology* 202, 1603–1623. 61
- Nigg, B.M., Bahlisen, H.A., Luethi, S.M., Stokes, S., 1987. The influence of running velocity and midsole hardness on external impact forces in heel-toe running. *Journal of Biomechanics* 20, 951–959. 63
- Nigg, B.M., Wakeling, J.M., 2001. Impact forces and muscle tuning: a new paradigm. *Exercise and Sport Science and Review* 29, 37–41. 65
- Patla, A.E., Prentice, S.D., Robinson, C., Neufeld, J., 1991. Visual control of locomotion: strategies for changing direction and for going over obstacles. *Journal of Experimental Psychology* 17, 603–634. 67
- Thigpen, M.T., Light, K.E., Creel, G.L., Flynn, S.M., 2000. Turning difficulty characteristics of adults aged 65 or older. *Physical Therapy* 80, 1174–1187. 69
- Walter, R.M., 2003. Kinematics of 90 degree running turns in wild mice. *Journal of experimental Biology* 206, 1739–1749. 71